LETTERS

# Radiative conductivity in the Earth's lower mantle

Alexander F. Goncharov[1], Benjamin D. Haugen[1,2], Viktor V. Struzhkin[1], Pierre Beck[1] & Steven D. Jacobsen[3]

**Iron in crustal and mantle minerals adopts several possible oxidation states: this has implications for biogeochemical processes[1], oxygenation of the atmosphere[2] and the oxidation state of the mantle[3,4]. In the deep Earth, iron in silicate perovskite, $(Mg_{0.9}Fe_{0.1})SiO_3$, and ferropericlase, $(Mg_{0.85}Fe_{0.15})O$, influences the thermal conductivity of the lower mantle and therefore heat flux from the core. Little is known, however, about the effect of iron oxidation states on transport properties. Here we show that the radiative component of thermal conductivity in the dominant silicate perovskite material of Earth's lower mantle is controlled by the amount of ferric iron, $Fe^{3+}$. We obtained the optical absorption spectra of silicate perovskite and ferropericlase at pressures up to 133 GPa, corresponding to pressures at the core–mantle boundary. Absorption spectra of ferropericlase up to 800 K and 60 GPa exhibit minimal temperature dependence. The results on silicate perovskite show that optical absorption in the visible and near-infrared spectral range is dominated by O–$Fe^{3+}$ charge transfer and $Fe^{3+}$–$Fe^{2+}$ intervalence transitions, whereas a contribution from the $Fe^{2+}$ crystal-field transitions is substantially smaller. The estimated pressure-dependent radiative conductivity, $k_{rad}$, from these data is 2–5 times lower than previously inferred from model extrapolations, with implications for the evolution of the mantle, such as generation and stability of thermo-chemical plumes in the lower mantle.**

The lower mantle extends from the 660-km seismic discontinuity to the core–mantle boundary at 2,900 km depth and constitutes roughly half of the Earth's mass. Dominated by just two silicate and oxide minerals—silicate perovskite and ferropericlase—the lower mantle controls the flow of latent and radiogenic heat out of the core, which contributes an estimated 25–30% of the total heat flux measured at the surface[5]. Thermal conductivity of the lower-mantle mineral assemblage therefore provides a constraint on the ability of the mantle to transfer heat non-convectively, but also influences convection[6]. The importance of temperature- and pressure-dependent thermal conductivity[7,8] has been recognized in recent geodynamic models of mantle convection, which incorporate variable thermal conductivity[9] and variable viscosity[6,10].

Thermal conductivity in metals is dominated by electron transport, whereas heat conduction in insulators (dielectrics) such as silicates and oxides is essentially dominated by vibrational (phonon) transport. At high temperature, thermal conductivity of mantle materials has a competing second contribution—radiative conductivity[7,11,12]. The radiative component of total conduction in defect-free material is determined by the material's optical properties, namely absorptivity. In silicates and oxides, direct photon transfer depends critically on the concentration and valence state of *d*-block elements, especially iron, whereas diffusive radiative transfer also depends on macroscopic properties, such as grain size[8]. Because the influence of transition metal elements such as iron on direct photon transfer is related to electronic structure, the spin state of iron is also an important factor in a material's infrared and visible spectral ranges where crystal-field transitions occur[13–15]. Application of laboratory-derived spectral data to conductivity in the lower mantle not only requires information on each component of heat transfer, but also their respective pressure and temperature dependencies[8].

Previous measurements of thermal diffusivity in mantle minerals at high pressures have been limited to the 5–10 GPa pressure range (that is, 150–300 km depth) at room temperature[16], with a few optical absorption studies of the direct radiative component of conductivity in olivine or silicate spinels at 20–30 GPa (refs 17, 18). At high temperatures, thermal diffusivity in olivine has been measured up to about 1,500 °C at ambient pressure[19]. At conditions deeper in the mantle and beyond previous experimental studies, theoretical models have been used to estimate pressure–temperature variation of thermal conductivity, but the validity of model predictions require experimental verification at conditions relevant to the lower mantle.

Optical absorption spectra of ferropericlase were recently reported to about 80 GPa at room temperature[20,21], and showed a strong dependence of absorptivity on iron concentration and pressure, and possibly on spin state. In ferropericlase, interpretation of optical spectra are complicated by the defect structure of (Mg,Fe)O, resulting from variable amounts of $Fe^{3+}$ in samples annealed at different conditions of oxygen fugacity and pressure[21]. Absorption spectra for Fe-bearing silicate perovskite have been reported[22,23], but so far only at ambient experimental pressure–temperature conditions.

The effect of pressure on optical absorption of Fe-bearing silicate perovskite is shown in Fig. 1. Observation of some bands requires thicker samples (>50 μm), which are difficult to accommodate in the diamond anvil cell at very high pressures (Supplementary Fig. 1). The crystal-field transition near 8,000 $cm^{-1}$ could not be detected with samples thinner than 15 μm. However, using an oil medium, we were able to study the sample of approximately 30 μm initial thickness to 46 GPa (Fig. 1a, Supplementary Fig. 1). Increasing pressure shifts the crystal-field band at 8,000 $cm^{-1}$ to higher energy, accompanied by a gradual decrease in absorption above about 36 GPa. Experiments in Ar media show that the crystal-field band becomes unobservable in the 43–84 GPa pressure range. However, the weakness of this band relative to the background in our spectra at high pressure prevents us from drawing definitive conclusions about whether this band disappears or falls below detection level. During the highest-pressure experiments, the crystal-field band was barely detectable (Fig. 1c) because thinner samples were used. Also, non-hydrostatic stresses, which develop within 'hard' pressure media (such as Ar at high pressure) or without a transmitting medium, are observed to broaden the crystal-field band, at least partly because of the increase in splitting between the individual components of the $^5E_g$–$^5T_{2g}$ transitions.

In agreement with the previous ambient pressure study[22], all three sets of measurements on silicate perovskite reveal a broad band near 15,000 $cm^{-1}$, with an ultraviolet absorption edge above 25,000 $cm^{-1}$ that has a broad absorption tail extending through the visible and near-infrared. The 15,000 $cm^{-1}$ band has previously been assigned to intervalence charge transfer[13,22,24]. Our measurements show a blue

[1]Geophysical Laboratory, Carnegie Institution of Washington, 5251 Broad Branch Road NW, Washington DC 20015, USA. [2]Department of Geological Sciences, University of Colorado, Boulder, Colorado 80309, USA. [3]Department of Earth and Planetary Sciences, Northwestern University, Evanston, Illinois 60208, USA.

shift of this band with pressure, similar to iron-bearing ringwoodite[18]. In perovskite, the intervalence band becomes sharper at approximately 40 GPa (Fig. 1a) and is almost invariant in frequency with increasing pressure above ~80 GPa. The ultraviolet absorption edge, which was assigned previously[22] to $O^{2-}$–$Fe^{3+}$ charge transfer, shows a moderate red shift (or increase of intensity) with pressure (Fig. 1). It has been argued[8] that this 'background' ultraviolet feature is due to grain boundary scattering. However, we also observe this feature in our single-crystal samples. Moreover, an Al-bearing perovskite crystal with 4% Fe also shows the ultraviolet absorption edge (Supplementary Fig. 1), which minimizes the likelihood that this band results from charged defects. We therefore tentatively assign the ultraviolet band to $O^{2-}$–$Fe^{3+}$ charge transfer, on the basis of the systematics of charge-transfer gap values in oxides[25]. However, we cannot exclude the possibility of a small contribution from the charge-transfer transition $O^{2-}$–$Fe^{2+}$. Ultraviolet–visible absorption is much smaller for samples with lower iron concentration (see Supplementary Information for detailed results), which confirms the proposed band assignments.

Relatively high radiative conductivity of the lower mantle has been inferred as a consequence of the high-spin to low-spin electronic transition of $Fe^{2+}$ in silicate perovskite and ferropericlase[14,15,26]. This conjecture draws from predictions of blue-shifting crystal-field transitions, which were believed to be the main mechanism of the absorption in the near-infrared and visible spectral ranges. As the thermal radiation corresponding to the Earth's lower mantle (2,200–3,000 K) has a maximum in the near-infrared, a blue shift would allow thermal radiation to propagate longer distances, thus increasing the radiative component of thermal conductivity. Our results show that this effect does occur in perovskite, but only over the pressure range up to ~50 GPa. The decrease in intensity of the $^5E_g$–$^5T_{2g}$ band at 7,000 $cm^{-1}$ (Fig. 1a, b) at 45–60 GPa is consistent with the pressure range of spin-pairing of $Fe^{2+}$ (refs 15, 27).

Because crystal-field transitions of $Fe^{3+}$ are much weaker (they are forbidden by spin conservation[13]) and because the intervalence $Fe^{2+}$–$Fe^{3+}$ optical transitions also change in the pressure range where the $^5E_g$–$^5T_{2g}$ transition diminishes (Fig. 1), we interpret the spectra with a spin transition of $Fe^{2+}$ in the dodecahedral (A) site in the 45–60 GPa range[15]. No other qualitative change in absorption is observed in our spectra (Fig. 1) above 60 GPa (compare ref. 15). The change in optical absorption near 50 GPa is rather subtle, being overwhelmed by other absorption mechanisms at higher pressures. Similarly to our previous results in ferropericlase[20] (see also Supplementary Fig. 2), at higher pressures we observe an increase in the absorption related to a red shift of the ultraviolet absorption edge, which causes an overall absorption increase that compensates or exceeds the effects of pressure on the crystal-field transitions. Unlike ferropericlase with high Fe concentration (>11%, which corresponds to the percolation limit), this increase of the absorption edge is rather moderate in silicate perovskite, so we assign it to the Fe–O charge transfer transitions (see also ref. 22). We observed a similar subtle change of the optical absorption in our 6% Fe (Mg,Fe)O samples[20].

The current results from optical absorption of silicate perovskite and ferropericlase (see also Supplementary Fig. 2) with iron concentrations relevant to Earth's lower mantle provide a basis for determining the direct radiative heat transfer of minerals over a wide depth range in the mantle. Although the effect of temperature on the absorption spectra of some minerals may be substantial[12], we do not expect this to be the case for silicate perovskite and ferropericlase, as the main absorption mechanisms are different to that in olivine studied in ref. 12. Our absorption measurements on 15% Fe (Mg,Fe)O samples to 60 GPa and 800 K did not show any substantial temperature dependence, which would affect the calculations of the radiative conductivity presented below (see Supplementary Fig. 3).

The radiative part of the thermal conductivity, $k_{rad}(T)$, can be calculated as follows[8]:

$$k_{rad}(T) = \frac{4}{3}\int_0^\infty \frac{\Lambda}{[1+\ln 10\Lambda\alpha(\nu,T)]} \times \frac{1}{\nu^2}\frac{\partial[n(\nu,T)^2(1-\exp(-\ln 10\Lambda\alpha(\nu,T)))I(\nu,T)]}{\partial T}\mathrm{d}\nu \quad (1)$$

where $I(\nu,T)$ is the Planck function ($T$ is temperature), $\nu$ is wavenumber, $n(\nu,T)$ is the refraction index, $\Lambda$ is the grain size (scattering length), and $\alpha$ is the measured absorption coefficient. Assuming the grain size is much larger than the typical absorption length (~$1/\alpha$), we have calculated the radiative contribution to thermal conductivity in the lower mantle (Fig. 2), using our experimental absorption spectra (Fig. 1, Supplementary Fig. 2).

Our estimated radiative conductivity is 2–5 times smaller than the previous report[7,8] based on extrapolations of mineral optical properties to higher pressures. Substantial contribution from the

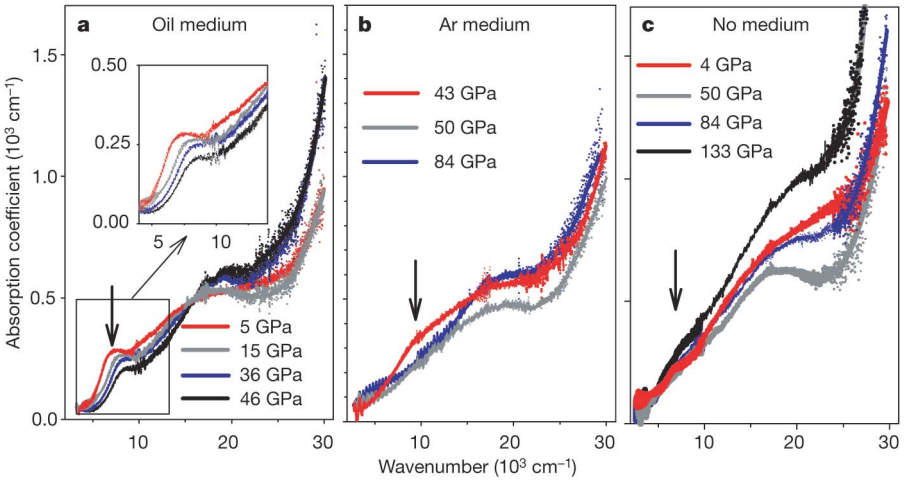


**Figure 1 | Optical absorption spectra of silicate perovskite (10 mol% Fe) up to 133 GPa at room temperature in various pressure media.** **a**, Oil; **b**, Ar, **c**, no medium. The absorption coefficient has been calculated using $\alpha = A\ln 10/d$, where $A = \log_{10}(I_0/I)$, $I_0$ and $I$ are the reference and sample signals respectively, and $d$ is the sample thickness measured from white-light interferometry at ambient pressure and calculated at high pressure using an isothermal equation of state. Although substantial care has been taken to measure $I_0$ and $I$ in the same conditions (for example, pressure), sample imperfections and limited sample dimensions affected the accuracy of the baseline, which has up to 50 $cm^{-1}$ uncertainty. Ripples in the spectra at low pressures are interference fringes resulting from multiple reflections between the parallel polished sample surfaces. The interference patterns and noisy spectral areas are smoothed (thick solid lines) for clarity. Vertical arrows designate the $Fe^{2+}$ crystal-field transitions, which are characteristic of the high-spin phase. Inset in **a** shows an enlarged view of the near-infrared spectral range (boxed).

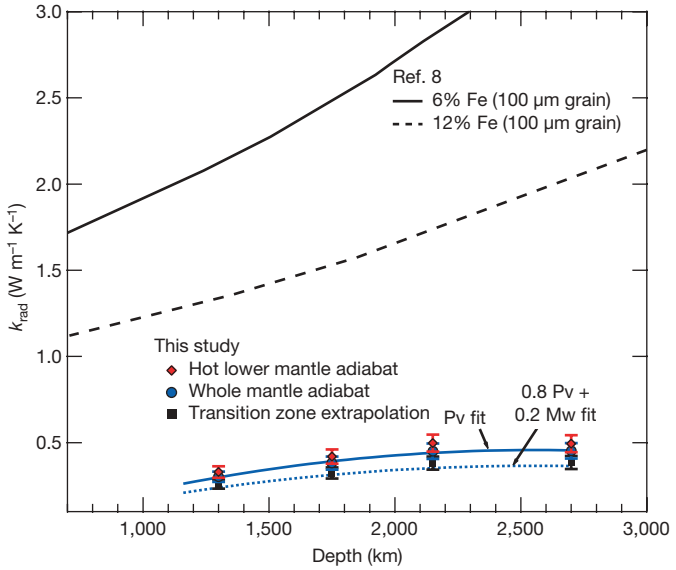


**Figure 2 | Radiative part of the Earth's lower-mantle thermal conductivity as a function of depth.** Three different geotherms were used, following ref. 8: a hot lower-mantle adiabat (red filled diamonds), a whole mantle adiabat (blue filled circles) and the extrapolated transition zone adiabat (black filled squares). Solid and dashed black lines present previous estimates of $k_{rad}$ for 6% and 12% iron concentrations, respectively[8]. The absorption coefficient was assumed to be temperature independent, which could have caused an overestimation of $k_{rad}$. We also suppose that the product $\alpha\Lambda$ is large ($\Lambda > 0.5$ mm). The radiative conductivity was calculated using equation (1) in two limiting cases: pure perovskite mantle (ferropericlase has a much larger absorption coefficient and therefore will not contribute to the diffusive radiative heat transfer) and a mixture of 80% of silicate perovskite, $(Mg_{0.9}Fe_{0.1})SiO_3$ and 20% of ferropericlase with 15% Fe composition (see Supplementary Information for the results in ferropericlase), which contribute proportionally (which would be valid in the case of the layered mantle). The results are shown as solid and dotted blue lines labelled 'Pv fit' and '0.8 Pv + 0.2 Mw fit', respectively. Error bars are projected uncertainties of the absorption coefficient measurements and their temperature corrections.

ultraviolet–visible absorption tails to the radiative conductivity, which could only be inferred in previous models[8], is responsible for the discrepancy. As absorption from the ultraviolet–visible tail is mostly due to the O–$Fe^{3+}$ charge transfer (see Supplementary Fig. 1), and the contribution from the $Fe^{2+}$–$Fe^{3+}$ intervalence charge transfer is substantial, the amount of the ferric iron in the mantle (that is, redox state) essentially controls the radiative heat conductivity (Fig. 2). According to our estimates, the radiative contribution does not exceed 0.54 W m$^{-1}$ K$^{-1}$ at the top of the D″ layer. The value of the thermal conductivity, $k$, in the thermal boundary layer strongly influences its thinness and stability: low values of $k$ typically imply a less stable and thinner boundary layer[28]. Moreover, a decrease in $k$ also implies a decrease in plume temperature[29]. These results should be taken into account when carrying out model calculations of the mantle dynamics[9,10,30]. Substantial efforts are still required to estimate the lattice contribution to thermal diffusivity at relevant pressures and temperatures.

## METHODS SUMMARY

**Sample preparation and characterization.** Single crystals of silicate perovskite were synthesized from synthetic $^{57}$Fe-enriched enstatite starting material ($En_{90}$) at 23 GPa and 1,800 °C. Electron microprobe analysis of the recovered samples confirmed the approximate chemical formula $(Mg_{0.9}Fe_{0.1})SiO_3$. Mössbauer spectroscopy indicates that 11 ± 3% of the iron is ferric ($Fe^{3+}$). Single-crystal structure refinements indicate that iron occupies the dodecahedral (A) site, without detectable iron in the octahedral (B) site (~2 mol% or less). For the optical absorption measurements at high pressures, samples were polished to 15–25 μm thickness and selected on the basis of their visible clarity. Silicate perovskite crystals exhibited sharp optical extinction in cross-polarized light, confirming their crystalline state.

**Optical absorption measurements.** Spectra were obtained in the 2,000–40,000 cm$^{-1}$ range using a custom infrared microscope and all-reflecting relay optics coupled to a Fourier-transform infrared spectrometer and a near-infrared-to-ultraviolet single-stage grating spectrograph with a CCD array detector. At each pressure, a spectrum through the sample and a spectrum through the pressure medium for background correction were obtained. A double confocal geometry was used to minimize scattered and spurious light, so the spectra of highly absorbing samples could be recorded.

**High-pressure techniques.** High-pressure measurements were carried out in a symmetric diamond anvil cell with various pressure media (Ar, Ne, silicone oil) to 87 GPa or without pressure medium (to 133 GPa).

**Received 5 July 2007; accepted 2 September 2008.**


1. Johnson, C. M. & Beard, B. L. Biogeochemical cycling of iron isotopes. *Science* **309,** 1025–1027 (2005).
2. Rouxel, O. J., Bekker, A. & Edwards, K. J. Iron isotope constraints on the Archean and Paleoproterozoic ocean redox state. *Science* **307,** 1088–1091 (2005).
3. McCammon, C. Perovskite as a possible sink for ferric iron in the lower mantle. *Nature* **387,** 694–696 (1997).
4. Frost, D. J. *et al.* Experimental evidence for the existence of iron-rich metal in the Earth's lower mantle. *Nature* **428,** 409–412 (2004).
5. Zhong, S. Constraints on thermochemical convection of the mantle from plume heat flux, plume excess temperature, and upper mantle temperature. *J. Geophys. Res.* **111,** B04409, doi:10.1029/2005JB003972 (2006).
6. Yanagawa, T. K. B., Nakada, M. & Yuen, D. A. Influence of lattice thermal conductivity on thermal convection with strongly temperature-dependent viscosity. *Earth Planets Space* **57,** 15–28 (2005).
7. Hofmeister, A. M. Mantle values of thermal conductivity and the geotherm from phonon lifetimes. *Science* **283,** 1699–1706 (1999).
8. Hofmeister, A. M. & Yuen, D. A. Critical phenomena in thermal conductivity: Implications for lower mantle dynamics. *J. Geodyn.* **44,** 186–199 (2007).
9. Dubuffet, F., Yuen, D. A. & Rainey, E. S. G. Controlling thermal chaos in the mantle by positive feedback from radiative thermal conductivity. *Nonlin. Process. Geophys.* **9,** 1–13 (2002).
10. van den Berg, A. P., Rainey, E. S. G. & Yuen, D. A. The combined influences of variable thermal conductivity, temperature- and pressure-dependent viscosity and core–mantle coupling on thermal evolution. *Phys. Earth Planet. Inter.* **149,** 259–278 (2005).
11. Clark, S. P. Jr. Radiative transfer in the Earth's mantle. *Trans. Am. Geophys. Union* **38,** 931–938 (1957).
12. Shankland, T. J., Nitsan, U. & Duba, A. G. Optical absorption and radiative heat transport in olivine at high temperature. *J. Geophys. Res.* **84,** 1603–1610 (1979).
13. Burns, R. G. *Mineralogical Applications of Crystal Field Theory* 2nd edn (Cambridge Univ. Press, 1993).
14. Sherman, D. M. The high-pressure electronic structure of magnesiowüstite (Mg,Fe)O: Applications to the physics and chemistry of the lower mantle. *J. Geophys. Res.* **96,** 14299–14312 (1991).
15. Badro, J. *et al.* Transitions in perovskite: Possible nonconvecting layers in the lower mantle. *Science* **305,** 383–386 (2004).
16. Ross, R. G., Andersson, P., Sundqvist, B. & Bäckström, G. Thermal conductivity of solids and liquids under pressure. *Rep. Prog. Phys.* **47,** 1347–1402 (1984).
17. Mao, H. K. & Bell, P. M. Electrical conductivity and the red shift of absorption in olivine and spinel at high pressure. *Science* **176,** 403–406 (1972).
18. Keppler, H. & Smyth, J. R. Optical and near infrared spectra of ringwoodite to 21.5 GPa: Implications for radiative heat transport in the mantle. *Am. Mineral.* **90,** 1209–1212 (2005).
19. Pertermann, M. & Hofmeister, A. M. Thermal diffusivity of olivine-group minerals at high temperature. *Am. Mineral.* **91,** 1747–1760 (2006).
20. Goncharov, A. F., Struzhkin, V. V. & Jacobsen, S. D. Reduced radiative conductivity of low-spin (Mg,Fe)O in the lower mantle. *Science* **312,** 1205–1208 (2006).
21. Keppler, H., Kantor, I. & Dubrovinsky, L. S. Optical absorption spectra of ferropericlase to 84 GPa. *Am. Mineral.* **92,** 433–436 (2007).
22. Keppler, H., McCammon, C. A. & Rubie, D. C. Crystal-field and charge-transfer spectra of $(Mg,Fe)SiO_3$ perovskite. *Am. Mineral.* **79,** 1215–1218 (1994).
23. Shen, G., Fei, Y., Hålenius, U. & Wang, Y. Optical absorption spectra of $(Mg,Fe)SiO_3$ silicate perovskites. *Phys. Chem. Miner.* **20,** 478–482 (1994).
24. Mattson, S. M. & Rossman, G. R. Identifying characteristics of charge transfer transitions in minerals. *Phys. Chem. Miner.* **14,** 94–99 (1987).
25. Bocquet, A. E. *et al.* Electronic structure of early 3*d*-transition-metal oxides by analysis of the 2*p* core-level photoemission spectra. *Phys. Rev. B* **53,** 1161–1170 (1996).
26. Badro, J. *et al.* Iron partitioning in Earth's mantle: Toward a deep lower mantle discontinuity. *Science* **300,** 789–791 (2003).
27. Li, J. *et al.* Pressure effect on the electronic structure of iron in $(Mg,Fe)(Si,Al)O_3$ perovskite: A combined synchrotron Mössbauer and X-ray emission spectroscopy study up to 100 GPa. *Phys. Chem. Miner.* **33,** 575–585 (2006).
28. Turcotte, D. L. & Schubert, G. *Geodynamics* (Cambridge Univ. Press, 2002).

29. Montague, N. L., Kellogg, L. H. & Manga, M. High-Rayleigh number thermo-chemical models of a dense boundary layer in D. *Geophys. Res. Lett.* **25,** 2345–2348 (1998).
30. Naliboff, J. B. & Kellogg, L. H. Can large increases in viscosity and thermal conductivity preserve large-scale heterogeneity in the mantle? *Phys. Earth Planet. Inter.* **161,** 86–102 (2007).

**Supplementary Information** is linked to the online version of the paper at www.nature.com/nature.

**Acknowledgements** We acknowledge support from NSF/EAR, DOE/BES, DOE/NNSA (CDAC) and the W. M. Keck Foundation. S.D.J. thanks D. J. Frost, S. J. Mackwell and D. P. Dobson for help with sample synthesis, C. A. McCammon for Mössbauer spectroscopy, J. R. Smyth for single-crystal X-ray diffraction, H. Watson for electron microprobe analysis of the silicate perovskite material and the NSF and Bayerishes Geoinstitut Visitor's Program for support. B.D.H. was supported by the NSF Research Experience for Undergraduates (REU) Program at the Carnegie Institution of Washington. P.B. was partially supported by the Balzan Foundation.

**Author Contributions** A.F.G., V.V.S. and S.D.J. designed the research programme; S.D.J. synthesized and polished the single crystals; A.F.G. and B.D.H. performed high-pressure experiments at room temperature; A.F.G., V.V.S. and P.B. performed high-temperature experiments; A.F.G., V.V.S., B.D.H. and P.B. analysed the data; P.B. developed a thermal conductivity model; V.V.S, A.F.G. and S.D.J interpreted the results; A.F.G, S.D.J., P.B. and V.V.S. wrote the paper. All authors discussed the results and commented on the manuscripts.

**Author Information** Reprints and permissions information is available at www.nature.com/reprints. Correspondence and requests for materials should be addressed to A.F.G. (goncharov@gl.ciw.edu).